Hierarchical Titania Nanotubes with Self-Branched Crystalline Nanorods

Changdeuck Bae,[‡,†] Youngjin Yoon,[†] Won-Sub Yoon,[†] Jooho Moon,[§] Jiyoung Kim,[||] and Hyunjung Shin*[,†]

National Research Lab for Nanotubular Structures of Oxides, Center for Materials and Processes of Self-Assembly, and School of Advanced Materials Engineering, Kookmin University, Jeongneung-Gil 77, Seoul 136-702, South Korea, Department of Materials Science and Engineering, Yonsei University, 262 Seongsanno, Seodaemun-gu, Seoul 120-749, South Korea, and Department of Materials Science and Engineering, University of Texas at Dallas, Richardson, Texas, 75083

ABSTRACT Surface decoration strategy for one-dimensional nanostructures will improve their electrical, optical, mechanical, and electrochemical performances dramatically. Heterogeneous growth/deposition on surfaces, however, may create undesired junction interfaces in the system. Here we report a procedure during which amorphous titania nanotubes are readily self-branched with crystalline titanate nanorods at room temperature. The starting amorphous titania nanotubes were prepared by low-temperature atomic layer deposition combined with the template-directed approach. We routinely observed the self-branching phenomenon of crystalline titanate nanorods with a few nanometers in diameter onto the surfaces of the amorphous titania nanotubes in mild alkali solutions. The resulting structures were analyzed by field-emission scanning electron microscopy, high-resolution transmission electron microscopy, and electron energy loss spectroscopy. The reactivity of the hierarchical titania nanotube arrays was observed to be improved as a Li secondary battery electrode. Upon complete consumption of the amorphous body of titania nanotubes, in addition, titanate nanosheets/layers consisting of single TiO_2 layers with unit-cell thickness were obtained, elucidating the formation mechanism of layered titanate materials by alkali treatment.

KEYWORDS: titania nanotubes • self-branching • Li secondary battery electrode • layered titanate.

INTRODUCTION

One-dimensional (1D) semiconducting nanostructures are at the heart of current research on nanometer scale science and technology. Recent reports highlight their use as efficient charge collectors with direct pathway in applications for renewable energy sources (1−3), energy scavenging (4, 5), and energy storage as batteries (6, 7). Although the distinct charge collection capabilities for individual 1D semiconducting nanostructures have been successfully demonstrated, the devices that can utilize the sum of 1D nanomaterials are still far from satisfactory. In many cases, this unsatisfactory situation is primarily due to the relatively lower roughness factors (dimensionless, defined as the total surface area per unit area of the devices) when compared to nanoporous counterparts (3). For example, photoanode arrays consisting of anodized titania nanotubes for application in dye-sensitized solar cells exhibited a superior electron diffusion length of ~100 μm in each nanotube (8), but their energy conversion efficiency (~7%, ref 9) did not exceed that of conventional nanoparticulate cells (~12%, ref 10). Consequently, to maintain the efficient 1D scaffold, increasing their specific surface area, so as to the roughness factor is the key. One possible approach would be introducing arms/branches on the surfaces of 1D nanostructured materials. However, heterogeneous growth/deposition onto the 1D nanostructures may create additional junction interfaces with electrical energy barriers (11, 12).

In 1998, Kasuga et al. reported for the first time that carbon nanotube-like TiO_2 nanotubes of ~8 nm in diameter can be reproducibly obtained by a strong alkali treatment of crystalline anatase TiO_2 powders (typically in a 10 M NaOH solution at 110 °C for ~20 h) (13). A number of studies followed to elucidate the formation mechanism of the extraordinary oxide nanotubes. By using high-resolution TEM, Zhou and Peng found that the Ti-containing oxide nanotubes are trititanate layered nanotubes (i.e., $H_2Ti_3O_7$) (14). Wang et al. proposed a formation process in which single atomic layer sheets of TiO_2 parallel with the (010) lattice planes are rolled up into nanotubular structures (15). Various experiments on structural control of the titania nanostructures, such as nanowires, nanosheets, and nanorods, under strong hydrothermal conditions, were reported and summarized in recent reviews (7). In spite of contradictory evidence in several experimental observations in terms of hydrogenation for lepidocrocite-TiO_2 (16), recent calculation results indicate that the ABA-stacked "step 3" $H_2Ti_3O_7$ compound is stable when the layered titanate is stacked to form (17, 18). However, the layered titanate structures

* Corresponding author. Tel: (82) 2 910 4897. Fax: (82) 2 910 4320. E-mail: hjshin@kookmin.ac.kr.

Received for review December 06, 2009 and accepted May 24, 2010

† Kookmin University.

‡ Present address: Institute of Applied Physics, University of Hamburg, Jungiusstrasse 11, 20355 Hamburg, Germany.

§ Yonsei University.

|| University of Texas at Dallas.

DOI: 10.1021/am100299e

studied so far were mostly produced from crystalline TiO_2 via homogeneous nucleation and growth in solutions. The exact origin from which the free-standing atomic layer sheets/patches being used as the building blocks of the nanotubes/layers is not clear at the current stage.

Herein we report an interesting phenomenon by which amorphous titania nanotubes, a model 1D semiconductor, are self-branched with crystalline titanate nanorods under mild alkali conditions, resulting in the enhancement of roughness factors of the system. The physical dimension and structures were characterized by field-emission scanning electron microscopy (FESEM), high-resolution transmission electron microscopy (HR-TEM), and electron energy loss spectroscopy (EELS). The geometry and growth selectivity were readily controlled, and the enhanced reactivity of the arrays of titania nanotubes of the hierarchical structures was also demonstrated as a Li secondary battery electrode. By demonstrating layered titanate structures obtained upon full consumption of the amorphous titania nanotubes, moreover, our results allow one to clearly elucidate the formation mechanism of layered titanate materials. The surface modification strategy reported here should open a new avenue for the utility of 1D functional nanomaterials with improved performance.

EXPERIMENTAL METHODS

Titania Nanotube Fabrication. Porous alumina membranes having the desired pore diameter were first prepared with the well-known two-step anodization method, or were commercially available (Anodisk, Whatman, U.K.). Amorphous titania layers were then deposited onto the alumina template by ALD at 120 °C. Titanium(IV) iso-propoxide (UP Chemical, Korea) and water vapor, respectively, were used as metal reactant and oxygen source. Ar was used as the carrier gas and also for the sake of purging. The total flow rate of the Ar was 250 sccm. The oxide layers were grown under 2.6 Torr.

Electrochemical Measurement. All electrochemical measurements were carried out using two-electrode cells. Galvanostatic cycling tests were performed using titania nanotubes as the working electrode. Li metal was used as the counter electrode. Glass membrane (Glass Micro Fiber, Whatman, UK) was used as a separator. The electrolyte was 1 M $LiPF_6$ in a 1:1 mixture of ethylene carbonate and dimethyl carbonate. No binders or conducting carbon were used. Cell assembly was conducted in an Ar-filled glovebox. Galvanostatic discharge−charge was performed using a Won-A Tech WBCS 3000 system; measuring potential was in a range of 0.7 to 3.0 V (Li^+/Li) at current rates from the *C*/20 to 600C ($1C$ = mA/g). The mass of TiO_2 nanotubes were measured directly using a microbalance (XR205SM-DR, with precision of 10 μg).

Sample Characterization. The geometry and dimensions of the resulting nanostructures were investigated by FESEM (JSM7000F, JEOL, Japan) and HRTEM (JEM2100F, JEOL, Japan). TEM samples were prepared by mechanically transferring the as-treated tubes onto a substrate and to a TEM grid.

RESULTS AND DISCUSSION

We used amorphous titania nanotubes as starting materials. These nanotubes were prepared by the template-directed low-temperature atomic layer deposition (ALD) method previously demonstrated by the authors (see also experimental section) (19). The wall thickness of the nanotubes can be precisely controlled by varying the number of ALD cycles of the desired oxide layer, and the length and diameter can be tailored according to the templates used (20, 21). Diameter modulation of the initial nanotubes is also possible simply by fabricating a diameter-modulated alumina membrane (22, 23). Upon the deposition of the TiO_2 layers, the as-deposited membranes were treated by immersion under mild alkali conditions, typically, 1−3 M NaOH (or KOH) at room temperature (up to 65 °C) for anywhere from several hours up to 72 h. Figure 1a shows the resulting hierarchical titania nanotubes after treatment with KOH (3 M) at room temperature followed by washing with pure water. The final diameter of ∼200 nm is comparable with the initial inner-pore diameter of the commercial alumina template used. Nanorodlike surface branches are apparent on the body of the tubular structures, as shown in Figure 1a. A similar phenomenon was observed in the experiments that used NaOH solutions (Figure 1b, and 3). In this case, alumina templates having sub-100 nm pore diameter were employed to demonstrate the similar roughness factor (up to∼1000) with that of the nanoporous counterparts, e.g., mesoporous particulate films (23). Figure 1b shows a TEM micrograph of the resultant self-branched structure from the amorphous titania nanotubes treated under a mild condition (1 M NaOH at 65 °C for ∼24 h). The original titania nanotubes had ∼60 nm diameter and ∼15 nm wall thickness. The reduced thickness of the nanotubes' wall in Figure 1b indicates consumption of the wall layers upon treatment. The essential feature is the branched nanotubular structures decorated with nanorodlike arms whose axis is nearly perpendicular to the tube axis, as observed in the KOH treatments (Figure 1a). Figure 1c shows an enlarged TEM image of a single branch 3−4 nm in diameter and a few tens of nanometers in length. Although the nanocrystalline nature of the branched nanotube was detected by the diffused electron diffraction result (the inset of Figure 1b), indistinct lattice fringes, in this particular case, might come from the off-axis of the layered structures. However, the presence of anatase (004) indicates that the atomic layers are stacked into the nanorods/sheets rather than forming quasi-2D rolls (15), as will be discussed later. To investigate these structures in detail, we recorded electron energy loss spectra (EELS) along the cross-sectional direction of the branched titania nanotube (Figure 1b, d). The core-loss EELS signal at the Ti L edges was recorded along line A−B in Figure 1b. Figure 1d shows the splitting and binding of peaks for the Ti L_3 and L_2 edges throughout the scanning, as marked by the empty black arrows. The complete crystal-field splitting on the Ti L edges is representative of the high quality of the local crystal symmetry (24). In addition to the electron diffraction data, therefore, the EELS line-scan results testify that the crystalline anatase TiO_2 branches were created from the amorphous body of titania nanotubes. The crystalline nature of the resulting titania is also characterized electrochemically in the Li secondary battery experiments, as will be shown in Figure 6.

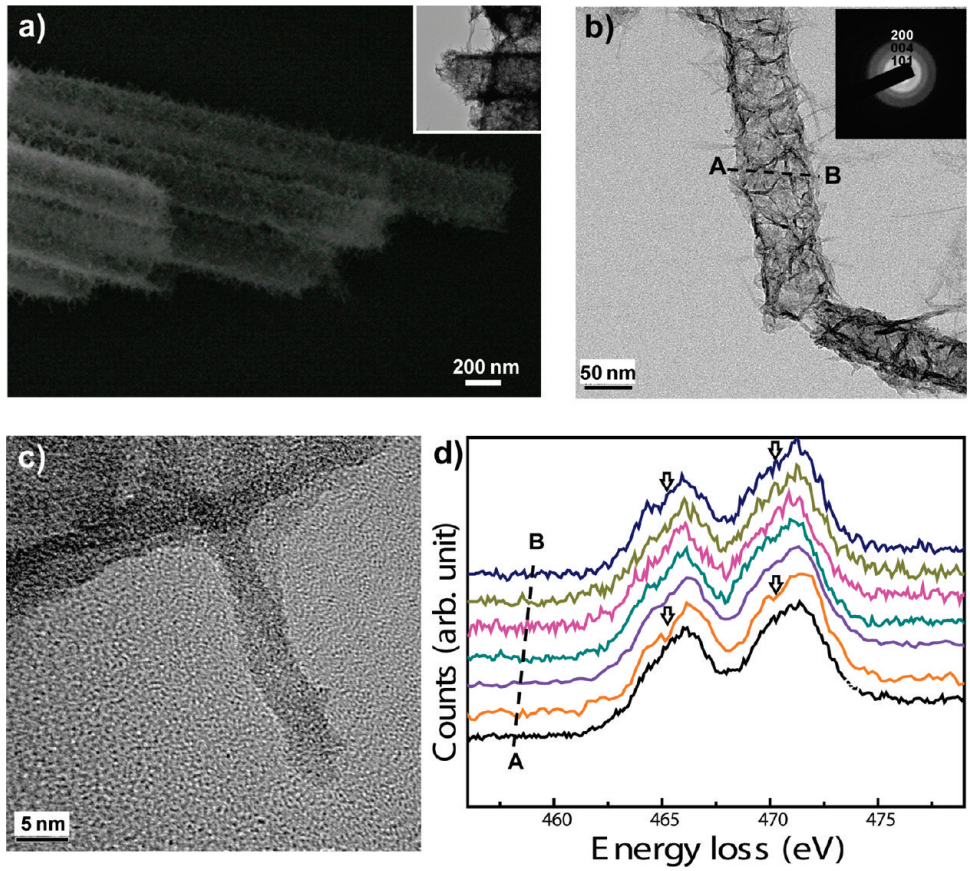

FIGURE 1. (a) Electron micrographs of the resulting branched structures after the alkali treatment of as-deposited amorphous nanotubes having 200 nm diameter and 20 nm wall thickness in a 3 M KOH solution at 25 °C for 72 h. The inset is the corresponding TEM image at the same magnification. (b) TEM images of the resulting structures after the alkali treatment of amorphous nanotubes possessing initial 60 nm diameter and 15 nm wall thickness in a 1 M NaOH solution at 65 °C for 24 h. The inset is the electron diffraction result from the tube of the panel b. (c) Magnified TEM image of a single branch. (d) Core-loss EELS spectra at the Ti L edges recorded along the line A−B in the panel b.

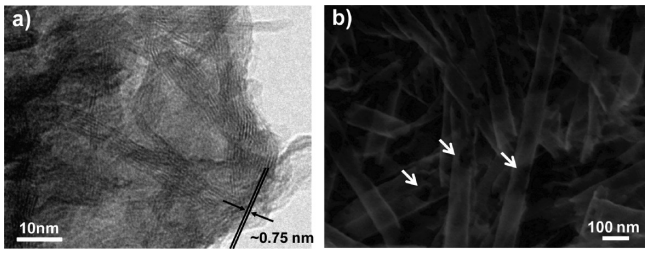

FIGURE 2. (a) TEM image of the titanate layers formed after complete consumption of the original amorphous titania nanotubes in the mild alkali solution. The nanotubular structures have gone and the nanolayers/sheets with ~0.75 nm interlayer spacing are seen in which there is no difference from those in the literature. (b) SEM image of the postannealed anatase TiO_2 nanotubes obtained after treatment with a strong alkali solution (10 M NaOH, 120 °C, 24 h). The original anatase TiO_2 nanotubes were prepared by depositing 15 nm thick amorphous titania layer inside homemade porous alumina templates having ~60 nm pore diameter, followed by annealing at 400 °C for 1 h. Upon the reaction, there is surface damage/dissolution (see the white arrowheads).

We further proceeded with the treatments and observed completely layered titanate sheets, as shown in Figure 2a, indicative of the full consumption of the body of amorphous titania nanotubes. The interlayer spacing was ~0.75 nm, which corresponds to that of the hydrotitanate layered structures (7). It should be noted that in a control experiment, no detectable branching was observed in the crystalline anatase TiO_2 nanotubes (i.e., those annealed at 400 °C for 1 h) upon the mild alkali treatment (1 M NaOH, 65 °C, 24 h), but the reaction with our anatase TiO_2 nanotubes under the typical strong hydrothermal condition (10 M NaOH, 120 °C, 24 h) resulted in significant surface damage/dissolution (see the white arrow heads, for example in Figure 2b). By comparing our results for the mild and strong alkali treatments, one can suspect that both treatments give rise to dissolved titania surfaces and provide the source of small TiO_x patches, but the dissolved patches seem to be branched only in the case of nanotubes with amorphous body (Figure 1a) and seem to be nucleated homogeneously for the anatase nanotubes (Figure 2b). A recent study of TiO_2 nanorod arrays on a Ti metal film also supports such an argument by demonstrating that an amorphous oxide or hydroxide layer formed on the Ti film can serve as a good adhesion layer between the strong alkali-treated nanorod arrays and the substrate (25).

Now, whether the branched titania is indeed from the amorphous body of titania nanotubes was investigated by observing the initial growth of the branches and by determining the formation mechanism. The amorphous nanotubes were prepared by depositing thin titania layers of ~20 nm onto the porous polycarbonate (PC, Whatman, UK) templates rather than using alumina with the same condi-

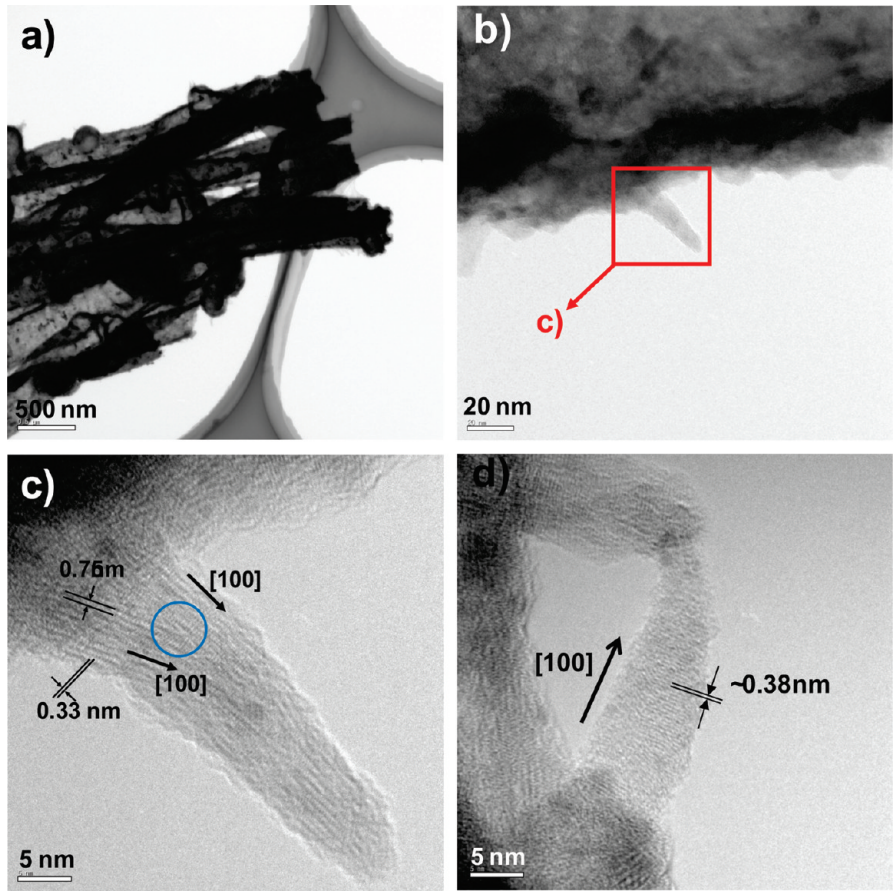

FIGURE 3. TEM micrographs of the titania nanotubes obtained from using the PC templates upon the mild alkali treatment (1 M NaOH, 65 °C) for ~1 h showing the initial stage of the branched growth of the hierarchical nanotubes. (a–d) TEM images at different magnifications, exhibiting that the branches are crystalline phase. The solid blue circle of panel c shows the merge of small crystalline segments, supporting the present growth mechanism.

tions, as mentioned above. In fact, alkali solutions such as NaOH and KOH are etchants for alumina, which means we cannot control the initial reaction time for the purposes of this experiment, and thus we chose the PC template. The resulting titania nanotubes were also amorphous, as previously reported by the authors (19). The mild alkali treatment was conducted with the amorphous titania nanotubes after complete dissolution of the PC template in a chloroform solution. Upon treatment with a 1 M NaOH solution at 65 °C for ~1 h, we observed the initial growth for the resulting structures. Figure 3 shows the initial structures of the self-branched titania nanotubes. Overall, sparse nanorods/branches are observed compared with the samples treated for more than ~20 h (Figure 1a). At an appropriate zone-axis, a crystalline branch with the stacked anatase (010) patches spaced by ~0.76 nm is clearly observed, as shown in Figure 3c. The spacing is equal to the interlayer distance between (010) planes for the layered TiO_2 structure. For the reason that the (010) planes were unit patches, we suspect the growth mechanism for this self-branch phenomena to be as follows. Both faces of the building blocks are mostly terminated with undercoordinated Ti_{5c} and O_{2c} atoms, and such dangling bonds are sensitive to ions in the alkali solutions. Therefore, the small TiO_x patches dissolved from the amorphous nanotube surfaces might be aligned and stacked into the anatase (010) planes, which are the most charge sensitive faces, growing to nanorods/sheets on the nanotube's surfaces (see the inset of Figure 1c). The perpendicular growth direction of this growth against the axis of the tube body (see for example, Figures 1a, b) might result from the repulsive interactions between the negatively charged building blocks during growth. The amorphous nanotubes of relatively good quality provided by the atomic layer-by-layer nature of ALD also seem to contribute to the success of the self-branching for the amorphous titania nanotubes. For example, electrochemically anodized titania surfaces might contain substantial fluorine-based complexes within the structures, and might be resistant to an alkali medium with different surface chemistry. Therefore, our amorphous nanotubes enable the system to hydrothermally react at low temperature, i.e., under mild alkali conditions.

Furthermore, the morphology and structure of the resulting hierarchical titania nanotubes can be controlled as, for example, in the following manner. Upon the above demonstration of crystal/amorphous (branch/body) nanotubes, all-crystalline, branched TiO_2 nanotubes were fabricated from the amorphous/anatase composite titania nanotubes that were prepared with high-temperature ALD (ca. 300 °C). In this case, the as-deposited titania nanotubes contain crystalline anatase grains in their interior and also have an amorphous phase as a result of the partial anatase nucleation and growth. Figures 4a–c show the TEM micrographs of the

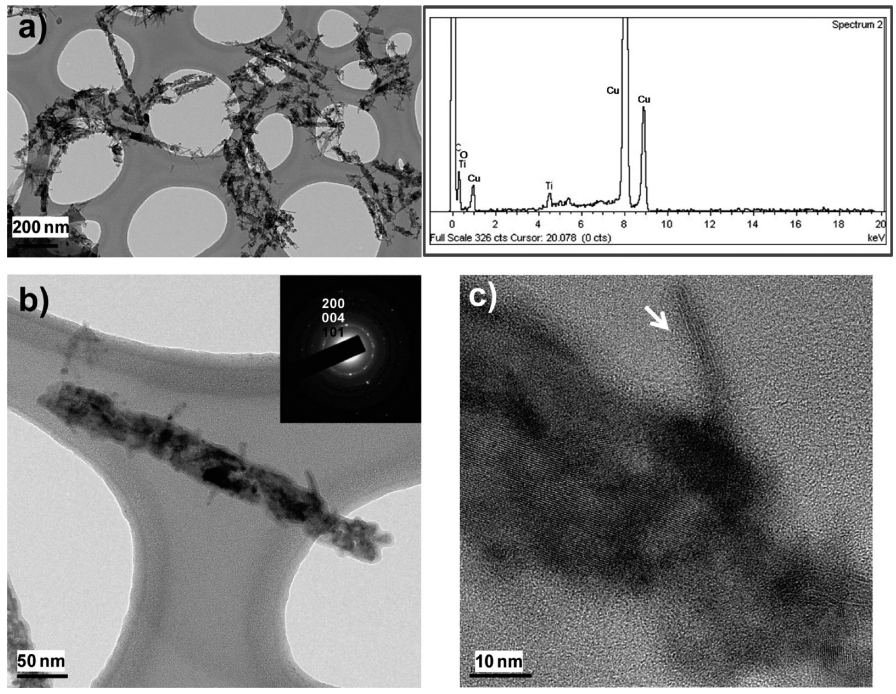

FIGURE 4. TEM images and representative EDX spectra of the hierarchical nanostructures branched from amorphous/anatase composite nanotubes. Enlarged TEM images show the individual and layered structures of the resulting branches.

resulting branched TiO_2 nanotubes. The as-deposited titania nanotubes were reacted for ~24 h in similar mild solutions, but the relatively short branches are probably a result of the small amount of amorphous matrix in the nanotube body, implying that the length of the branches can be tailored by controlling the amorphous contents of the titania nanotubes. The layered structures of the nanorod branch were also observed in the magnified TEM image shown in Figure 4c, in which the crystalline anatase lattice fringe of the tube body is seen supporting the self-branched nanorod/arm.

The branches can be also created on the desired surfaces of nanotubes in a site-selective manner by using the template material itself as a delay agent during wet chemical etching. Alumina templates housing amorphous titania nanotubes coated conformally in their interior, i.e., in-house samples, were plunged into the mild alkali solutions without removal of the template. After at least one day (up to one week), the samples were washed with pure water and were observed as shown in Figures 5a–c. Figure 5a displays top-view SEM micrographs showing inside nanotubes at the relatively initial stage of growth after partial etching of surfaces (i.e., mechanical polishing). White arrowheads in Figure 5a indicate the branched structures inside the tube. Typical TEM images b and c in Figure 5, taken after 2–3 days, testify that the inner surfaces are mostly branched (see the inset of panel a). In these experiments, the inner surfaces of the nanotubes were first exposed to the alkali solutions and branched until there was a complete dissolution of the template materials. Therefore, it was sufficient to control the branching kinetics between the inner and outer surfaces of the amorphous titania nanotubes. Interestingly, after such long-term treatment under mild conditions, the branches

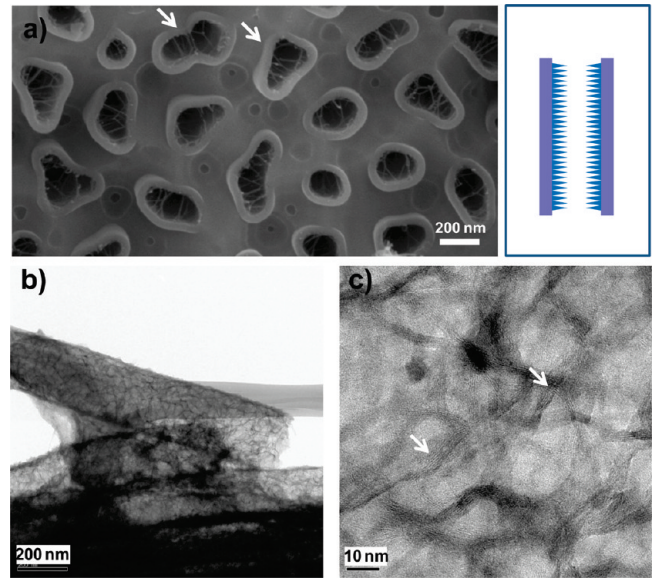

FIGURE 5. (a) SEM micrographs of the partially etched surfaces of the inner surface-branched titania nanotubes at the relatively initial reaction stage, showing the branched nanorods inside the pores as indicated by the white arrows. The right-side scheme illustrates the inner-surface-branched tubular structure. (b, c) TEM of the only inner-surface-branched hierarchical titania nanotubes upon the desired reaction time in which the layered structures are seen as pointed-out by the white arrowhead.

grew into layered structures (Figure 5b,c, see the white arrow of panel c), as seen by others in typical strong alkali treatments.

The increased surface area and crystalline nature of the resulting self-branched TiO_2 nanotubes were experimentally demonstrated by electrochemical characterization. The arrays of TiO_2 nanotubes before and after the mild alkali treatment were compared as electrodes in lithium batteries. Array structures of tubular titania on Cu metal supports were

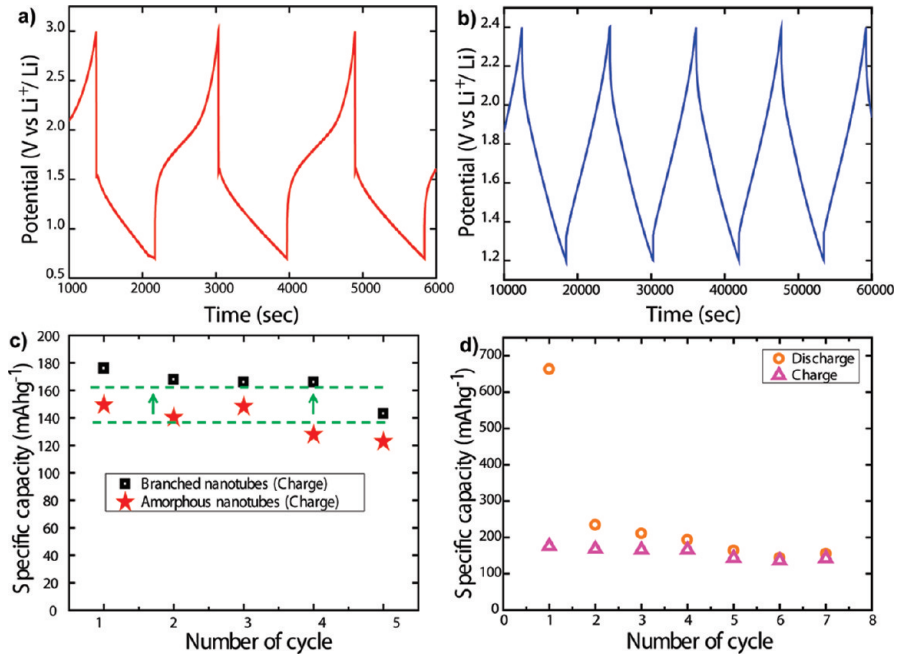

FIGURE 6. (a) Galvanostatic discharge/charge curves of the branched TiO_2 nanotube arrays, showing the semivoltage plateau, and (b) those of the amorphous TiO_2 nanotube arrays as a control. (c) Comparison of the specific capacity between the branched and nonbranched (as-prepared) nanotube arrays on several cycling test. The green dotted lines and arrowheads indicate the increased specific capacity upon branching. (d) Capacity evolution versus cycle number for the branched TiO_2 nanotube anodes.

prepared by methods reported previously by the authors (20). Panels a and b in Figure 6 show a comparison of the galvanostatic discharge/charge curves of the two. As for the branched structures, the essential feature was the presence of the semivoltage plateau in the curves, which is indicative of insertion and deinsertion of Li ion from specific sites of crystalline structures, such as tetrahedral and octahedral sites, in the case of the tetragonal anatase structure (26). We suspect that the semivoltage plateau might result from the superimposition of the electrochemical performances of amorphous and crystalline anodes, implying the successful self-branching of crystalline arms from the amorphous body at room temperature. A recent study of the electrochemical characterization of anodized TiO_2 surfaces with/without postannealing supports our argument (27). The results for the cycling of the two samples, i.e., before and after branching, testify to the increased specific surface that leads to the enhanced device performance (the inset of Figure 6c). The active surface area was observed to be improved by ~20% in terms of the specific capacity of the Li secondary battery, as indicated by the green arrows in Figure 6c. The stability and rate capability require further study in order to use such a material in high-performance Li batteries (28, 29).

CONCLUSIONS

In summary, we report a self-branching phenomenon from amorphous titania nanotubes to hierarchical nanorod-branched titania nanotubes in diluted alkali solutions at near room temperature. This mild hydrothermal reaction provides a simple, versatile way to create hierarchical 1D nanostructures without extrinsic junction interfaces. The amorphous titania nanotubes prepared by the template-directed low-temperature ALD are believed to allow for the successful reaction. Layered titanate structures consisting of single-layer TiO_2 sheets, obtained upon full consumption of the amorphous titania nanotubes, indicate that our branched structures are in an intermediate state in the formation of layered titanate materials by strong alkali treatment. The surface modification strategy reported here should have the potential for improved electrical and electrochemical applications, as demonstrated in the application of this system for a Li secondary battery anode.

Acknowledgment. We acknowledge financial support from the NRL Programs (R0A-2007-000-20105-0), the Nano R&D Program (M10503000255-05M0300-25510, 2005-02522, 2009-0082717), Priority Research Centers Program (2009-0093814), Mid-career Researcher Program through NRF grant funded by the MEST (Nos. 2009-0086302), and the CMPS (R11-2005-048-00000-0) of MEST/KOSEF.

REFERENCES AND NOTES

(1) Huynh, W. U.; Dittmer, J. J.; Alivisatos, A. P. *Science* **2002**, *295*, 2425.
(2) Law, M.; Greene, L. E.; Johnson, J. C.; Saykally, R.; Yang, P. *Nat. Mater.* **2005**, *4*, 455.
(3) Tian, B.; Zheng, X.; Kempa, T. J.; Fang, Y.; Yu, N.; Yu, G.; Huang, J.; Lieber, C. M. *Nature* **2007**, *449*, 885.
(4) Hochbaum, A. I.; Chen, R.; Delgado, R. D.; Liang, W.; Garnett, E. C.; Najarian, M.; Majumdar, A.; Yang, P. *Nature* **2008**, *451*, 163.
(5) Qin, Y.; Wang, X. D.; Wang, Z. L. *Nature* **2008**, *451*, 809.
(6) Armstrong, A. R.; Armstrong, G.; Canales, J.; García, R.; Bruce, P. G. *Adv. Mater.* **2005**, *17*, 862.
(7) Bavykin, D. V.; Friedrich, J. M.; Walsh, F. C. *Adv. Mater.* **2006**, *18*, 2807.
(8) Jennings, J. R.; Ghicov, A.; Peter, L. M.; Schmuki, P.; Walker, A. B. *J. Am. Chem. Soc.* **2008**, *130*, 13364.
(9) Varghese, O. K.; Paulose, M.; Grimes, C. A. *Nat. Nanotechnol.* **2009**, *4*, 592.

(10) Grätzel, M. *Inorg. Chem.* **2005**, *44*, 6841.
(11) (a) Wang, D.; Qian, F.; Yang, C.; Zhong, Z.; Lieber, C. M. *Nano Lett.* **2004**, *4*, 871. (b) Jung, Y.; Ko, D.-K.; Agarwal, R. *Nano Lett.* **2007**, *7*, 264.
(12) (a) Milliron, D. J.; Hughes, S. M.; Cui, Y.; Manna, L.; Li, J.; Wang, L.-W.; Alivisatos, A. P. *Nature* **2004**, *430*, 190. (b) Cui, Y.; Banin, U.; Björk, M. T.; Alivisatos, A. P. *Nano Lett.* **2005**, *5*, 1519.
(13) (a) Kasuga, T.; Hiramatsu, M.; Hoson, A.; Sekino, T.; Niihara, K. *Langmuir* **1998**, *14*, 3160. (b) Kasuga, T.; Hiramatsu, M.; Hoson, A.; Sekino, T.; Niihara, K. *Adv. Mater.* **1999**, *11*, 1307.
(14) Chen, Q.; Zhou, W.; Du, G. H.; Peng, L.-M. *Adv. Mater.* **2002**, *14*, 1208.
(15) Yao, B. D.; Chan, Y. F.; Zhang, X. Y.; Zhang, W. F.; Yang, Z. Y.; Wang, N. *Appl. Phys. Lett.* **2003**, *82*, 281.
(16) Wang, W.; Varghese, O. K.; Paulose, M.; A Grimes, C.; Wang, Q.; Dickey, E. C. *J. Mater. Res.* **2004**, *19*, 417.
(17) Enyashin, A. N.; Seifert, G. *Phys. Status Solidi B* **2005**, *242*, 1361.
(18) Casarin, M.; Vittadini, A.; Selloni, A. *ACS Nano* **2009**, *3*, 317.
(19) Shin, H.; Jeong, D.-K.; Lee, J.; Sung, M. M.; Kim, J. *Adv. Mater.* **2004**, *16*, 1197.
(20) Bae, C.; Yoo, H.; Kim, S.; Lee, K.; Kim, J.; Sung, M. M.; Shin, H. *Chem. Mater.* **2008**, *20*, 756.
(21) Bae, C.; Kim, S.; Ahn, B.; Kim, J.; Sung, M. M.; Shin, H. *J. Mater. Chem.* **2008**, *18*, 1362.
(22) Bae, C.; Kim, H.; Han, D.; Yoo, H.; Kim, J.; Shin, H. *Small* **2009**, *5*, 1936.
(23) Bae, C.; Yoon, Y.; Yoo, H.; Han, D.; Cho, J.; Lee, B. H.; Sung, M. M.; Lee, M.; Kim, J.; Shin, H. *Chem. Mater.* **2009**, *21*, 2574.
(24) Brun, N.; Colliex, C.; Rivory, J.; Yu-Zhang, K. *Microsc. Microanal. Microstruct.* **1996**, *7*, 161.
(25) Miyauchi, M.; Tokudome, H.; Toda, Y.; Kamiya, T.; Hosono, H. *Appl. Phys. Lett.* **2006**, *89*, 43114.
(26) Koudriachova, M. V.; Harrison, N. M.; de Leeuw, S. W. *Phys. Rev. B: Condens. Mater* **2002**, *65*, 235423.
(27) Ortiz, G. F.; Hanzu, I.; Djenizian, T.; Lavela, P.; Tirado, J. L.; Knauth, P. *Chem. Mater.* **2009**, *21*, 63.
(28) Simon, P.; Gogotsi, Y. *Nat. Mater.* **2008**, *7*, 845.
(29) Bruce, P. G.; Scrosati, B.; Tarascon, J.-M. *Angew. Chem., Int. Ed.* **2008**, *47*, 2.

AM100299E